

Understanding Heavy Quarkonium Production at Hadron Collider

Zhi-Guo He

II. Institut für Theoretische Physik, Universität Hamburg

Based on Collaboration with Kniehl et al.

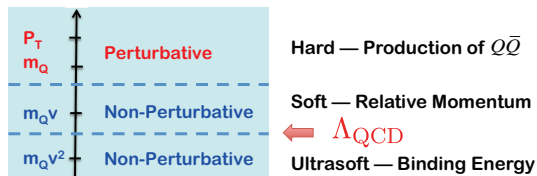
Phys.Rev.Lett. 115,022002, Phys.Rev.Lett. 121,172001 and ArXiv:1901.XXXXX

24.12.2018, UCAS, Beijing

- 1 Introduction
- 2 Double J/ψ hadroproduction in collinear parton model
- 3 Double J/ψ hadroproduction in Parton Reggeization Approach
- 4 Breakdown of NRQCD in Processes Involving 2 Quakonia and its Cure

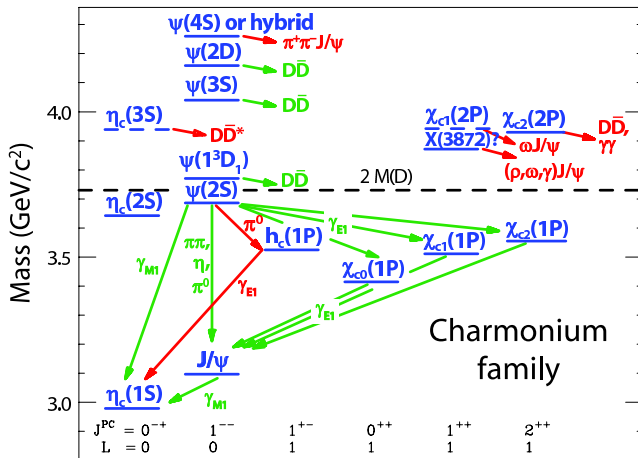
What is heavy quarkonium?

- Heavy quarkonium is one of the simplest QCD bound state constituted by heavy quark pair $Q\bar{Q}$ ($m_Q \gg \Lambda_{QCD}$).
- It is labeled by the spectroscopic notation $n^{2S+1}L_J$.
 - Its parity $P = (-1)^{L+1}$.
 - Its charge conjugation parity $C = (-1)^{L+S}$.
- There are 3 typical energy scales besides Λ_{QCD} :

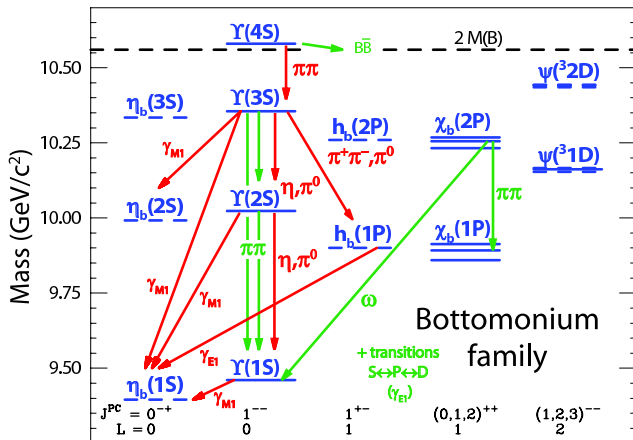


- It is an approximately non-relativistic system:
 - Charmonium: $v^2 \approx 0.23 \ll 1$
 - Bottomonium: $v^2 \approx 0.08 \ll 1$

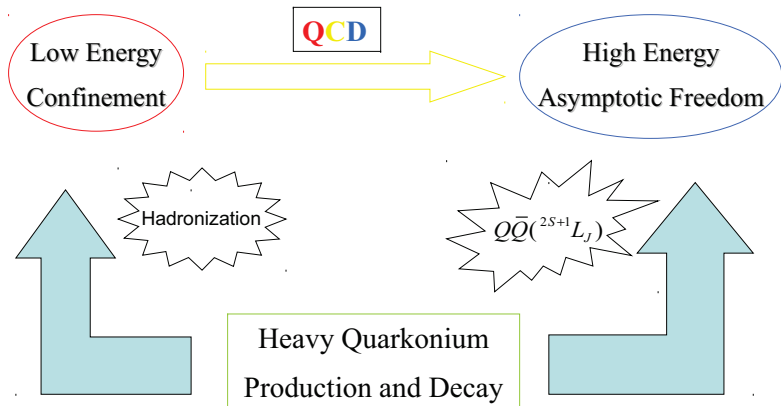
Charmonium family



Bottomonium family



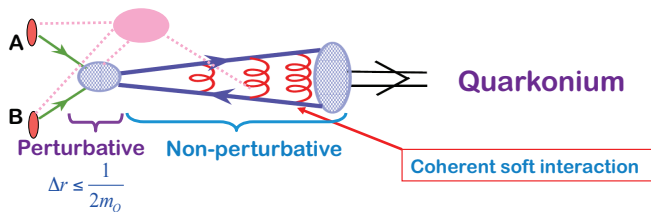
Why are we interested in heavy quarkonium production?



J/ψ and Υ are ideal candidates for their large leptonic branching functions!

The picture of heavy quarkonium production

- $A + B \rightarrow \text{Quarkonium} + X$



- General Factorization Formula

$$\sigma_{(A+B \rightarrow J/\psi + X)} = \sum_n \int \sigma_{A+B \rightarrow (c\bar{c})_n + X} \times f[(c\bar{c})_n \rightarrow J/\psi]$$

Color Singlet Model

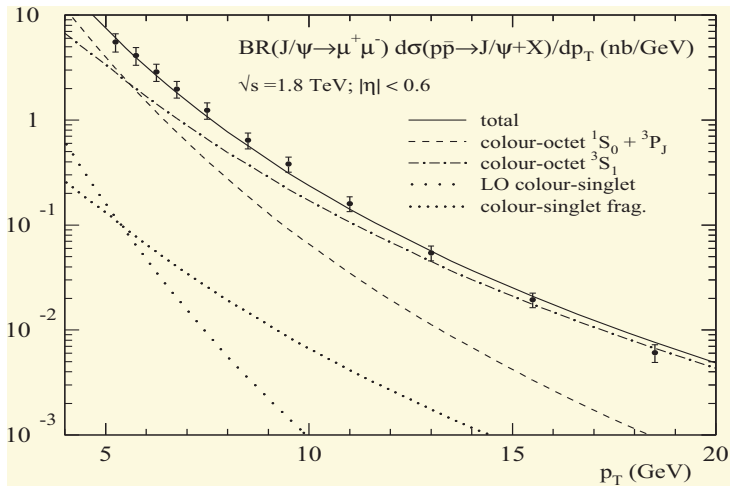
- Short Distance Part: The produced $Q\bar{Q}$ pair shares **the same quantum number** as the heavy meson.
- Long Distance Part: The non-relativistic wave function or its derivatives at origin.
- Non-factorizable in production and decay: S-wave relativistic corrections, P-wave at v^2 LO.

NRQCD Factorization Approach

- Short Distance Part: The produced $Q\bar{Q}$ pair can be **any possible quantum numbers**, even in **color octet**.
- Long Distance Part: The relative size of contribution from each Fock state obeys velocity scaling rules.
- The infrared divergence is absorbed into the QCD corrections to the long distance matrix elements.

CSM VS. NRQCD @ QCD LO

- Comparison between CSM and NRQCD predictions at QCD LO with CDF measurements for p_t distribution of direct J/ψ production:

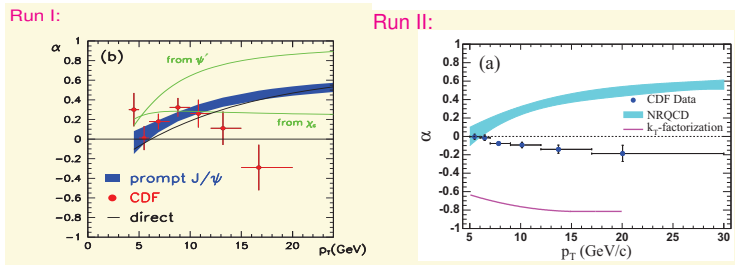


The “ J/ψ polarization puzzle” at LO

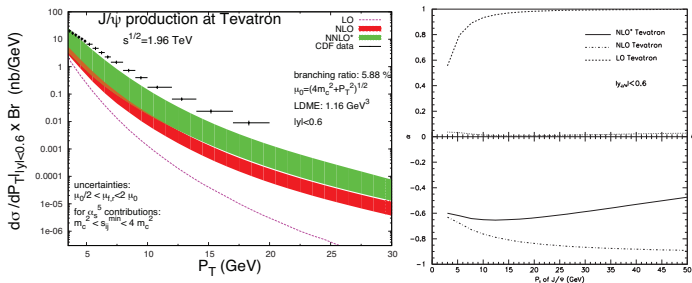
- The polarization of J/ψ is measured through the angular distribution of l^+l^- in its decay.

$$\frac{d\sigma}{d\cos\theta} \propto 1 + \alpha \cos\theta$$

- NRQCD Predictions @ LO:



- Comparison between CSM predictions at QCD NLO with CDF measurements for yield (left) and polarization (right) of prompt J/ψ production:

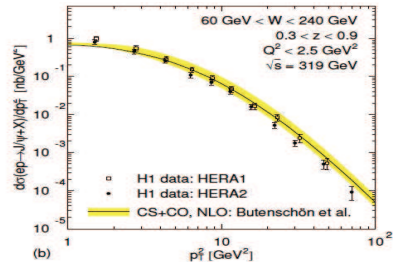
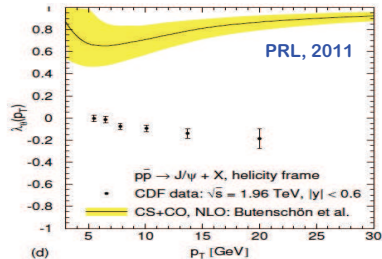
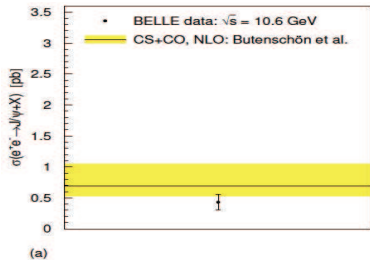
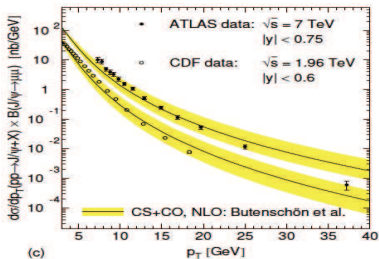


At QCD NLO, the CSM can neither explain J/ψ yield nor polarization distribution!! 😞

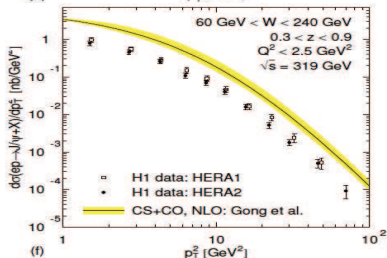
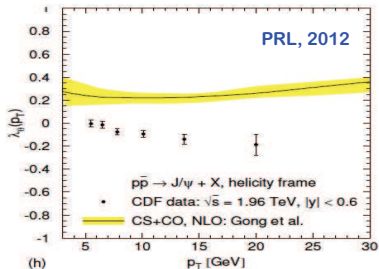
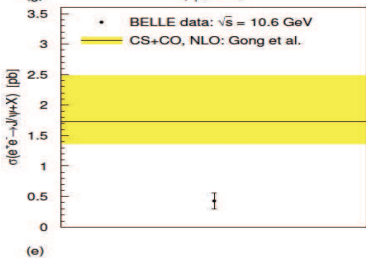
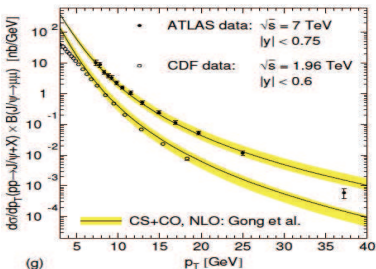
- SDCs: The SDCs for both yield and polarization including χ_c feed-down contribution were calculated by 3 groups independently. They are all in agreement with each other.
- Different sets of long-distance matrix elements (LDMEs) are obtained by fitting the SDCs @ QCD NLO to experimental data under different considerations, which lead to completely different conclusions.

	Butenschön, Kniehl [4]	Chao, Ma, Shao, Wang, Zhang [6]	Gong, Wan, Wang, Zhang [7]
$\langle \mathcal{O}^{J/\psi}({}^3S_1^{[1]}) \rangle / \text{GeV}^3$	1.32	1.16	1.16
$\langle \mathcal{O}^{J/\psi}({}^1S_0^{[8]}) \rangle / \text{GeV}^3$	0.0304 ± 0.0035	0.089 ± 0.0098	0.097 ± 0.009
$\langle \mathcal{O}^{J/\psi}({}^3S_1^{[8]}) \rangle / \text{GeV}^3$	0.0016 ± 0.0005	0.0030 ± 0.012	-0.0046 ± 0.0013
$\langle \mathcal{O}^{J/\psi}({}^3P_0^{[8]}) \rangle / \text{GeV}^5$	-0.0091 ± 0.0016	0.0126 ± 0.0047	-0.0214 ± 0.0056
$\langle \mathcal{O}^{\chi_0}({}^3P_0^{[1]}) \rangle / \text{GeV}^5$			0.107
$\langle \mathcal{O}^{\chi_0}({}^3S_1^{[8]}) \rangle / \text{GeV}^3$			0.0022 ± 0.0005

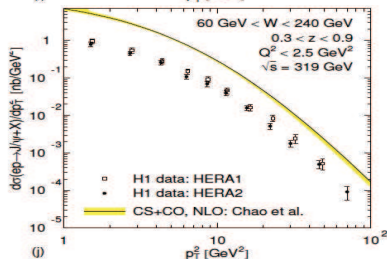
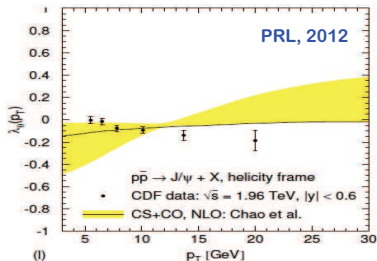
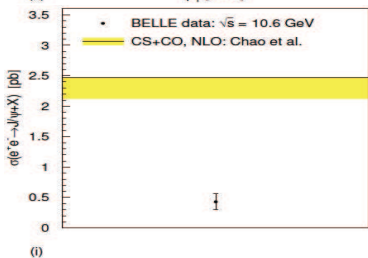
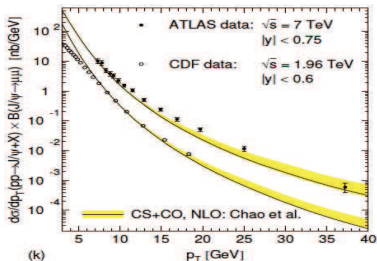
The results of Kniehl group



The results of Wang's group

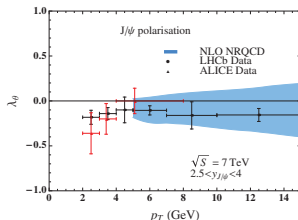
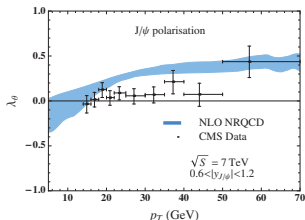
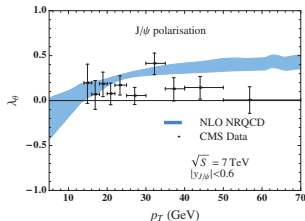
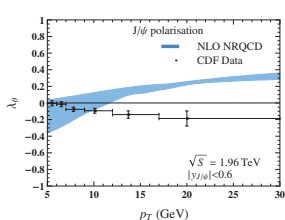


The results of Chao's group



The results of Chao's group updated

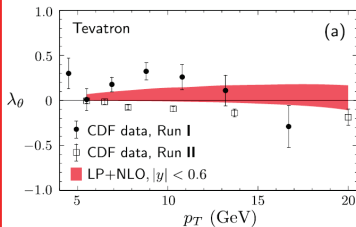
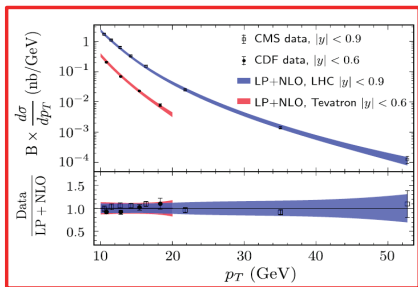
- Only the 2 combinations of three LDMEs, $M_{0,3.9} = (7.4 \pm 1.9) \times 10^{-2}$, $M_{0,0.56} = (0.05 \pm 0.02) \times 10^{-2}$ were obtained by fitting Tevatron yield data (Shao et al. 2015).



The results of other approach

- The LDMEs were also determined independently by fitting the fragmentation calculation to J/ψ hadroproduction data (Bodwin et al. 2014) yielding that

$$\langle \mathcal{O}^{J/\psi}(1S_0^{[8]}) \rangle = 0.099 \pm 0.022 \text{ GeV}^3, \langle \mathcal{O}^{J/\psi}(3S_1^{[8]}) \rangle = 0.011 \pm 0.010 \text{ GeV}^3, \langle \mathcal{O}^{J/\psi}(3P_0^{[8]}) \rangle = 0.011 \pm 0.010 \text{ GeV}^5.$$



Double J/ψ production from theoretical point of view

- In double J/ψ production, the hadronization of charm quark pair takes twice. Therefore, it provides an particularly sensitive test on NRQCD hypothesis.
- The double J/ψ production also provides an additional crucial constrain on the J/ψ LDMEs.
- It is believed that double J/ψ can be produced also through double parton scattering (DPS) mechanism, which can help to extract the parameters in DPS (Kom, et al. 2011, Baranov, et al. 2013).

Theoretical study of double quarkonium hadroproduction I

- Studying the double J/ψ production was first proposed by Barger, et al. in 1996, in which the $2(c\bar{c}(^3S_1^{[8]}))$ contribution was studied.
- Later, it is found that the CS $2(c\bar{c}(^3S_1^{[1]}))$ channel contributes predominately to the total hadroproduction rate (Qiao 2002).
- In 2013, Li, et al. calculated the relativistic corrections to both channels mentioned above.
- Recently the next-to leading QCD corrections to the $2(c\bar{c}(^3S_1^{[1]}))$ channel is obtained by Sun et al. in 2016.

Theoretical study of double quarkonium hadroproduction II

- Production of double heavy quarkonia other than double J/ψ are also studied, such as, double η_c (Li, et al. 2009), $J/\psi + \Upsilon$ (Ko, et al. 2011), $J/\psi + \eta_c + X$ (Lansberg, et al. 2013)
- Investigation of SPS+DPS contribution to double quarkonium production @LHC and after@LHC has also been performed (Lansberg et al. 2015).
- The double quarkonium production also is studied in the framework of k_t factorization (Baranov 2015).
- And more ...

Experimental measurements for double J/ψ hadroproduction

- Double J/ψ is first measured by LHCb Collaboration at 7 TeV in the rapidity range of $2.0 < y^{J/\psi} < 4.5$ and $p_T^{J/\psi} < 10\text{GeV}$ updated recently at 13 TeV LHC (LHCb 2012,2017).
- It is also measured by D0 Collaboration at 1.96 TeV with $p_T^{J/\psi} > 4\text{GeV}$ and $|\eta^{J/\psi}| < 2.0$, where the single parton scattering (SPS) and DPS contributions are discriminated (D0 2014).
- The CMS Collaboration measure double J/ψ production in details with cut condition shown in page 31 of this talk (CMS 2014).
- The double J/ψ production in central rapidity range $|y^{J/\psi}| < 2.1$ with higher cut on J/ψ p_t ($p_T^{J/\psi} > 8.5\text{GeV}$) was measured by ATLAS Collaboration at 8 TeV LHC (ATLAS 2017).

NRQCD factorization formula for prompt double J/ψ production

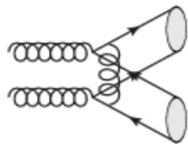
$$\begin{aligned} d\sigma(AB \rightarrow 2J/\psi + X) &= \sum_{i,j,m,n,H_1,H_2} \int dx_1 dx_2 \\ &\times f_{i/A}(x_1) f_{j/B}(x_2) d\hat{\sigma}(ij \rightarrow c\bar{c}(m)c\bar{c}(n) + X) \\ &\times \langle \mathcal{O}^{H_1}(m) \rangle \text{Br}(H_1 \rightarrow J/\psi + X) \times \langle \mathcal{O}^{H_2}(n) \rangle \text{Br}(H_2 \rightarrow J/\psi + X), \end{aligned}$$

At LO, $J/\psi + \chi_c$ sub-processes are forbidden because of the charge conjugation conservation, so there are in all $7 \times 8/2 - 3 = 25$ sub-processes needed to be calculated.

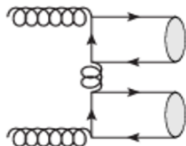
Note

The $q\bar{q}$ process is highly suppressed, so we only focus on the gluon-gluon fusion process.

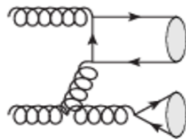
The topological properties of the Feynman diagrams



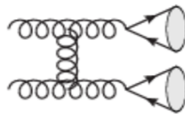
[a]



[b]



[c]



[d]

4-type of Feynman diagrams:

- a) Non-fragmentation type-I
- b) Non-fragmentation type-II
- c) Single fragmentation like
- d) Double fragmentation like

Power counting for each channel at large p_T

According to the scaling $d\sigma/dp_T^2 \propto 1/p_T^N$ and the topological properties of the Feynman diagrams, the partonic sub-processes can also be divided into 4 categories:

- 1 NNLP-I, with $N = 8$, including $m = {}^3S_1^{[1]}$ and $n = {}^3S_1^{[1,8]}, {}^1S_0^{[8]}, {}^3P_J^{[8]}$;
- 2 NNLP-II, with $N = 8$, too, including $m, n = {}^1S_0^{[8]}, {}^3P_J^{[8]}, {}^3P_J^{[1]}$;
- 3 NLP, with $N = 6$, including $m = {}^3S_1^{[8]}$ and $n = {}^1S_0^{[8]}, {}^3P_J^{[8]}, {}^3P_J^{[1]}$; and
- 4 LP, with $N = 4$, including $m = n = {}^3S_1^{[8]}$.

Note

While the NNLP-I and NNLP-II subprocesses exhibit the same p_T scaling, they differ by the topologies of the respective Feynman diagrams. In the latter case, these are the diffraction-like ones as in Fig. (b), which allow for large values of $|\Delta y|$ and thus for an enhancement of the cross section at large values of J/ψ pair invariant mass $m_{J/\psi}$.

The p_T and v^2 behaviors for each channel

- Together with the velocity scaling rule of NRQCD LDMEs and assuming that the branch function is also of v^2 order, we can obtain the p_T and v^2 scaling of $d\sigma/dp_T^2$ for the relevant pairings (m, n) of $c\bar{c}$ Fock states of each $gg \rightarrow c\bar{c}(m)c\bar{c}(n)$ channel.

(m, n)	$^3S_1^{[1]}$	$^3S_1^{[8]}$	$^1S_0^{[8]}$	$^3P_J^{[8]}$	$^3P_J^{[1]}$
$^3S_1^{[1]}$	$1/p_T^8$	v^4/p_T^8	v^3/p_T^8	v^4/p_T^8	0
$^3S_1^{[8]}$	—	v^8/p_T^4	v^7/p_T^6	v^8/p_T^6	v^8/p_T^6
$^1S_0^{[8]}$	—	—	v^6/p_T^8	v^7/p_T^8	v^7/p_T^8
$^3P_J^{[8]}$	—	—	—	v^8/p_T^8	v^8/p_T^8
$^3P_J^{[1]}$	—	—	—	—	v^8/p_T^8

The numerical inputs

Corresponding LDMEs in units of GeV^3 (Braaten, et al. 2000)

$$\begin{aligned} \mathcal{O}^{J/\psi}(^3S_1^{[1]}) &= 1.16, \quad \mathcal{O}^{J/\psi}(^3S_1^{[8]}) = 3.9 \times 10^{-3}, \quad M_{3.4}^{J/\psi}(^1S_0^{[8]}) = 6.6 \times 10^{-2}, \\ \mathcal{O}^{\psi'}(^3S_1^{[1]}) &= 0.758, \quad \mathcal{O}^{\psi'}(^3S_1^{[8]}) = 3.7 \times 10^{-3}, \quad M_{3.5}^{\psi'}(^3S_1^{[1]}) = 7.8 \times 10^{-3}, \\ \mathcal{O}^{\chi_{c0}}(^3P_0^{[1]})/m_c^2 &= 4.77 \times 10^{-2}, \quad \text{and } \mathcal{O}^{\chi_{c0}}(^3S_1^{[8]}) = 1.9 \times 10^{-3}. \end{aligned}$$

PDF, α_s and scale settings

One-Loop running of α_s^4 with $\Lambda^4 = 192 \text{ MeV}$, and CTEQ5L pdf.

$$\mu_r = \mu_f = m_T = \sqrt{(4m_c)^2 + p_T^2}.$$

Branch functions from higher states to J/ψ (PDG2012)

$$\begin{aligned} \text{Br}(\chi_{c1} \rightarrow J/\psi\gamma) &= 33.9\%, \quad \text{Br}(\chi_{c2} \rightarrow J/\psi\gamma) = 19.2\%, \quad \text{and} \\ \text{Br}(\psi' \rightarrow J/\psi + X) &= 60.9\%. \end{aligned}$$

General features of numerical results

- Among the NNLP-I subprocesses, compared to the CS^* no kinematic enhancements are found in other channels, so the other channels are all suppressed at least by $\mathcal{O}(v^3)$.
- Although the p_T scalings of the NNLP-II subprocesses is the same as the NNLP-I ones, the SDCs of these channels can be 50–200 times larger than that of the CS^* .
- The contribution of the NLP subprocesses can also exceed that of the CS^* channel.
- The CS^* channel contributes predominately in low invariant mass region, when $m_{J/\psi J/\psi}$ is much larger than $2 m_{J/\psi}$, the contribution of the NNLP-II, NLP,LP subprocesses can be orders of magnitude larger than that of the CS^* channel.
- From the identical-boson symmetry and $J/\psi + \chi_{cJ}$ suppression, the relative importance of the χ_{cJ} ($\psi(2S)$) feed-down contribution is reduced (enhanced) compared to single J/ψ production case.

The measured cross section

$$\sigma_{\text{tot}}^{\text{LHCb}} = (5.1 \pm 1.0 \pm 1.1) \text{ nb.}$$

LO $\text{CS}^* + \text{CO}^*$ prediction

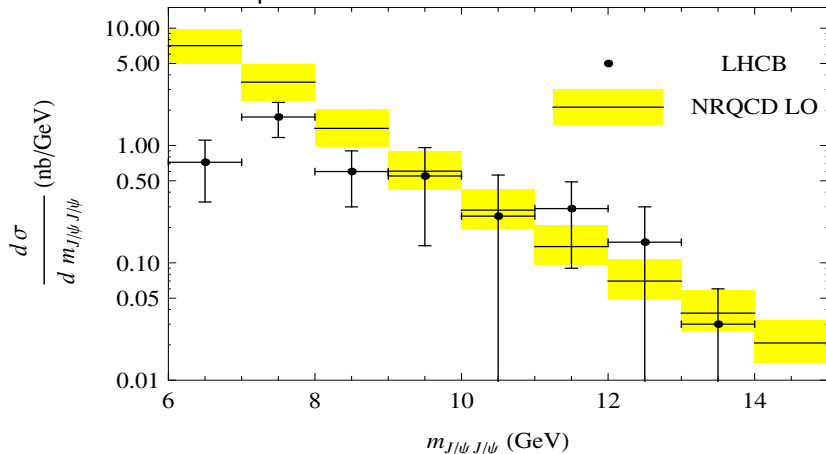
$$\sigma_{\text{tot}}^* = 12.2_{-3.8}^{+4.8} \text{ nb.}$$

Complete LO prediction

$$\sigma_{\text{tot}} = 13.2_{-4.1}^{+5.2} \text{ nb,}$$

which is about 2.6 times larger than the LHCb result.

- The invariant mass spectrum:



The measured cross section

$$\sigma_{\text{SPS}}^{\text{D0}} = (70 \pm 6 \pm 22) \text{ fb}, \quad \sigma_{\text{DPS}}^{\text{D0}} = (59 \pm 6 \pm 22) \text{ fb}.$$

LO CS* prediction

$$\sigma_{\text{tot}}^* = 51.9 \text{ fb}.$$

- Complete LO result can enhance that of the LO CS* by around 28%, which yields a nice agreement between NRQCD and D0 measurement.

NRQCD predictions meet CMS measurements I

- The CMS kinematic cut conditions:

$$\begin{aligned} p_T^{J/\psi} &> 4.5 \text{ GeV} && \text{if } 1.43 < |y^{J/\psi}| < 2.2, \\ 4.5 \text{ GeV} < p_T^{J/\psi} < 6.5 \text{ GeV} && \text{if } 1.2 < |y^{J/\psi}| < 1.43, \\ p_T^{J/\psi} > 6.5 \text{ GeV} && \text{if } |y^{J/\psi}| < 1.2. \end{aligned}$$

The measured cross section:

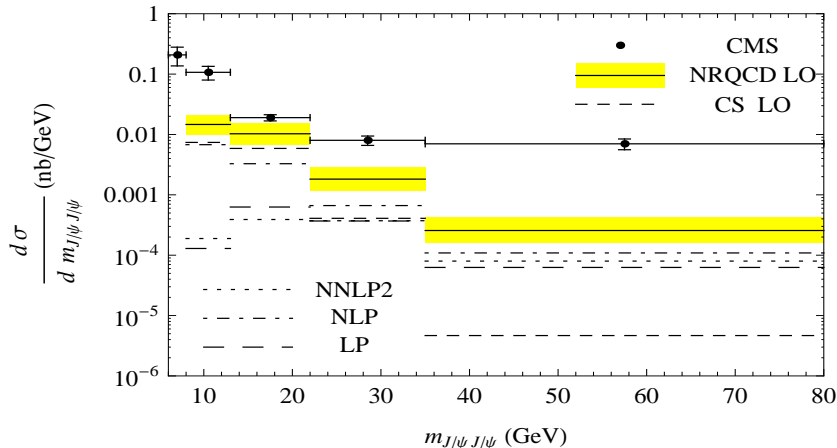
$$\sigma_{\text{tot}}^{\text{CMS}} = (1.49 \pm 0.07 \pm 0.13) \text{ nb.}$$

CPM prediction

$$\sigma_{\text{tot}}^{\text{LO}*} = 0.10_{-0.03}^{+0.05} \text{ nb}, \sigma_{\text{CS}}^{\text{NLO}*} = 0.98 \pm 0.16 \text{ nb. } \sigma_{\text{tot}}^{\text{LO}} = 0.15_{-0.05}^{+0.08} \text{ nb.}$$

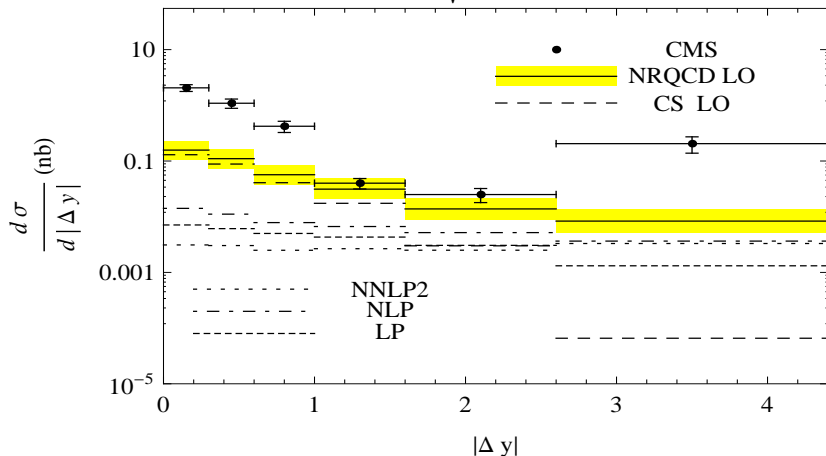
NRQCD predictions meet CMS measurements II

- The invariant mass spectrum:



NRQCD predictions meet CMS measurements III

- The $|\Delta y|$ distribution ($m_{J/\psi J/\psi} = 2\sqrt{4m_c^2 + p_T^2 \text{Cosh}(\Delta y)}$):



- The double J/ψ hadroproduction is first complete studied within NRQCD factorization formulism, which include all the possible combinations of CS and CO channels and the contribution of χ_{cJ} and $\psi(2S)$ mesons feed-down as well.
- The NRQCD prediction agrees well with the D0 data.
- The NRQCD prediction is about 2.6 times larger than the LHCb measurements, where the difference comes from the threshold region.
- There are orders of magnitude discrepente between NRQCD predictions and CMS measurements in large invariant mass and $|\Delta y|$ bins.

Why the parton Reggeization Approach? I

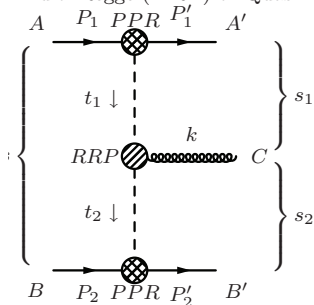
- The $p_T^{\psi\psi}$ distribution of CMS measurements indicates the predominant contribution comes from the $2 \rightarrow 3$ partonic processes in CPM calculation.
- The complete NLO QCD corrections are much more complicated.
- This problem can be partially overcome by the k_T factorization approach, in which the initial partons carry non-zero transverse momentum.
- In the old- k_t factorization approach the polarization, $\epsilon^\mu(q)$, of the initial gluon with 4-momentum $q = (q_0, \mathbf{q}_T, q_z)$ is described by $\epsilon^\mu(q) = \frac{q_T^\mu}{|\mathbf{q}_T|}$, but such formalism is not gauge invariant.

Why the parton Reggeization Approach? II

- This problem can be resolved by Reggeization of the amplitudes in QCD.
- In fact, for the hard part of the double J/ψ production the characteristic scale $\mu \approx \sqrt{(4m_c)^2 + (p_T^{\psi\psi})^2}$ satisfies $\Lambda_{QCD} \ll \mu \ll \sqrt{S}$, which implies accessing a new dynamical regime, namely the high-energy Regge limit.
- In such regmime, the NLO QCD corrections can be largely embodied by the \mathbf{p}_T un-integrated PDF in PRA.
- In single quarkonium production case, the PRA predictions agree well with the experimental data. (for example, Kniehl 2006)

Reggeization of amplitudes in QCD

PRA is based on the Reggeization of amplitudes in gauge theories (QED, QCD, Gravity). The *high energy asymptotics* of the $2 \rightarrow 2 + n$ amplitude is dominated by the diagram with t -channel exchange of the effective (Reggeized) particle and Multi-Regge (MRK) or Quasi-Multi-Regge Kinematics (QMRK) of final state.



In the limit $s \rightarrow \infty$, $s_{1,2} \rightarrow \infty$, $-t_1 \ll s_1$, $-t_2 \ll s_2$ (Regge limit), $2 \rightarrow 3$ amplitude has the form:

$$\mathcal{A}_{AB}^{A'B'C} = 2s \gamma_{A'A}^{R_1} \left(\frac{s_1}{s_0} \right)^{\omega(t_1)} \frac{1}{t_1} \times \\ \times \Gamma_{R_1 R_2}^C(q_1, q_2) \times \frac{1}{t_2} \left(\frac{s_2}{s_0} \right)^{\omega(t_2)} \gamma_{B'B}^{R_2}$$

$\Gamma_{R_1 R_2}^C(q_1, q_2)$ - RRP effective production vertex,

$\gamma_{A'A}^R$ - PPR effective scattering vertex,

$\omega(t)$ - Regge trajectory.

Two approaches to obtain this asymptotics:

- BFKL-approach (Unitarity, renormalizability and gauge invariance), see e. g. [Ioffe, Fadin, Lipatov, 2010].
- Effective action approach [Lipatov, 1995].

The effective Lagrangian for PRA I

To produce the amplitudes for the arbitrary QMRK processes, the effective-action approach is very useful. Light-cone coordinates and derivatives:

$$n^+ = \frac{2P_2}{\sqrt{S}}, \quad n^- = \frac{2P_1}{\sqrt{S}}, \quad n^+ n^- = 2$$
$$x^\pm = n^\pm x = x^0 \pm x^3, \quad \partial_\pm = 2 \frac{\partial}{\partial x^\mp}$$

Lagrangian of the effective theory $L = L_{kin} + \sum_y (L_{QCD} + L_{ind})$, $v_\mu = v_\mu^a t^a$,

$[t^a, t^b] = f^{abc} t^c$. The rapidity space is sliced into the subintervals, corresponding to the groups of final-state particles, close in rapidity. Each subinterval in rapidity ($1 \ll \eta \ll Y$) has its own set of QCD fields:

$$L_{QCD} = -\frac{1}{2} \text{tr} [G_{\mu\nu}^2], \quad G_{\mu\nu} = \partial_\mu v_\nu - \partial_\nu v_\mu + g [v_\mu, v_\nu].$$

Different rapidity intervals communicate via the gauge-invariant fields of Reggeized gluons ($A_\pm = A_\pm^a t^a$) with the kinetic term:

$$L_{kin} = -\partial_\mu A_+^a \partial^\mu A_-^a,$$

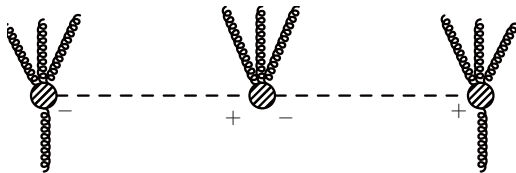
and the kinematical constraint:

$$\partial_- A_+ = \partial_+ A_- = 0 \Rightarrow$$

$$A_+ \text{ has } k_- = 0 \text{ and } A_- \text{ has } k_+ = 0.$$



The effective Lagrangian for PRA II



Particles and Reggeons interact via *induced interactions*:

$$L_{ind} = -tr \left\{ \left(\frac{1}{g} \partial_+ U [v^+] \right) \cdot \partial_\sigma \partial^\sigma A_-(x) + \left(\frac{1}{g} \partial_- U [v^-] \right) \cdot \partial_\sigma \partial^\sigma A_+(x) \right\}$$

$$U [v^\pm] = P \exp \left(-\frac{g}{2} \int_{-\infty}^{x^\mp} dx'^\mp v_\pm(x') \right)$$

Wilson lines generate the infinite chain of the induced vertices:

$$L_{ind} = tr \left\{ \left[v_+ - g v_+ \partial_+^{-1} v_+ + g^2 v_+ \partial_+^{-1} v_+ \partial_+^{-1} v_+ - \dots \right] \partial_\sigma \partial^\sigma A_- + \left[v_- - g v_- \partial_-^{-1} v_- + g^2 v_- \partial_-^{-1} v_- \partial_-^{-1} v_- - \dots \right] \partial_\sigma \partial^\sigma A_+ \right\}$$

The Feynman rules I

- $R^{+,a} \rightarrow Q + \bar{Q}$

$$i g_s T^a \gamma^+$$

- $R^+(k_1, a) + R^-(k_2, b) \rightarrow g(k_1 + k_2, \mu, c)$

$$-2 g_s f_{abc} \left(\left(\frac{k_2^2}{k_1^+} + k_2^- \right) n_+^\mu - \left(\frac{k_1^2}{k_2^-} + k_1^+ \right) n_-^\mu + (k_1 - k_2)^\mu \right)$$

The Feynman rules II

- $R^+(k_1, a) \rightarrow g(p_1, \mu_1, c) + g(k_1 - p_1, \mu_2, c)$

$$\begin{aligned} & - g_s f_{abc} (n_-^{\mu_2} (p_1 - 2k_1)^{\mu_1} + n_-^{\mu_1} (k_1 + p_1)^{\mu_2}) \\ & + \frac{k_1^2 n_-^{\mu_1} n_-^{\mu_2}}{p_1^-} - 2g^{\mu_1 \mu_2} p_1^- \end{aligned}$$

- $R^+(k_1, a) + R^-(k_2, b) \rightarrow g(p_1, \mu_1, c) + g(p_2, \mu_2, d)$

$$\begin{aligned} & -i g_s^2 (n_+^{\mu_1} n_-^{\mu_2} (f_{abe} f_{cde} + f_{ace} f_{bde}) - n_-^{\mu_1} n_+^{\mu_2} (f_{abe} f_{cde} - f_{ade} f_{bce})) \\ & - \frac{2k_1^2 n_-^{\mu_1} n_-^{\mu_2} (p_1^- f_{abe} f_{cde} - k_2^- f_{ace} f_{bde})}{k_2^- p_1^- p_2^-} - 2g^{\mu_1 \mu_2} (f_{ade} f_{bce} + f_{ace} f_{bde}) \\ & + \frac{2k_2^2 n_+^{\mu_1} n_+^{\mu_2} (p_1^+ f_{ace} f_{bde} + p_2^+ f_{ade} f_{bce})}{k_1^+ p_1^+ p_2^+} \end{aligned}$$

Factorization formula in PRA

Similar to the CPM, we ignore the contribution of $q\bar{q}$ channel.

$$d\sigma(AB \rightarrow 2J/\psi + X) = \sum_{m,n,H_1,H_2} \int \frac{dx_1}{x_1} \int \frac{d^2\mathbf{q}_{T_1}}{\pi} \int \frac{dx_2}{x_2} \int \frac{d^2\mathbf{q}_{T_2}}{\pi} \\ \times \Phi_{R^+/A}(x_1, |\mathbf{q}_{T_1}|^2, \mu^2) \Phi_{R^-/B}(x_2, |\mathbf{q}_{T_2}|^2, \mu^2) d\hat{\sigma}(R^+R^- \rightarrow c\bar{c}(m) + c\bar{c}(n)) \\ \times \langle \mathcal{O}^{H_1}(m) \rangle \text{Br}(H_1 \rightarrow J/\psi + X) \times \langle \mathcal{O}^{H_2}(n) \rangle \text{Br}(H_2 \rightarrow J/\psi + X),$$

where

$$d\hat{\sigma}(R^+R^- \rightarrow c\bar{c}(m) + c\bar{c}(n)) = \frac{\overline{|\mathcal{M}|^2}_{PRA}}{2S_{x_1x_2}} d \text{LIPS}$$

with

$$\overline{|\mathcal{M}|^2}_{PRA} = \frac{1}{8^2} \left(\frac{q_1^+ q_2^-}{4|\mathbf{q}_{T_1}||\mathbf{q}_{T_2}|} \right)^2 \sum_{color, spin} |\mathcal{M}|^2_{PRA}$$

Relations with CPM Calculation

- The number of the sub-processes is the same as in CPM calculation and for each one the corresponding Feynman diagrams can be obtained by changing the initial gluons gg to R^+R^- .
- Relation between pdfs.

$$\int dt \Phi_{R/A}(x, t, \mu^2) = x f_{g/A}(x, \mu^2)$$

- Relation between matrix elements,

$$\lim_{|\mathbf{q}_{T1,2}| \rightarrow 0} \int_0^{2\pi} \frac{d\phi_1 d\phi_2}{(2\pi)^2} |\overline{\mathcal{M}}|^2_{PRA} = \frac{1}{2^{28} 2} \sum_{color, spin} |\overline{\mathcal{M}}|^2_{CPM}$$

- The collinear limit for all the channels is checked analytically.

Topological properties of the Feynman diagrams

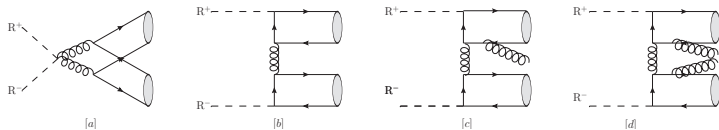


FIG. 1: Typical Feynman diagrams for $R^+ R^- \rightarrow c\bar{c}(m) c\bar{c}(n)$
 (a) non-t-channel gluon exchange type, (b) t-channel gluon exchange type at α_s LO, (c) t-channel gluon exchange type at α_s NLO, (d) t-channel gluon exchange type at α_s NNLO.

3-categories of partonic subprocesses:

- ① LT, including $m = 1 S_0^{[8]}, 3 S_1^{[8]}, 3 P_J^{[1,8]}$ and $n = 1 S_0^{[8]}, 3 S_1^{[8]}, 3 P_J^{[1,8]}$.
- ② NLT, including $m = 3 S_1^{[1]}$ and $n = 1 S_0^{[8]}, 3 S_1^{[8]}, 3 P_J^{[1,8]}$.
- ③ NNLT, including $m = 3 S_1^{[1]}$ and $n = 3 S_1^{[1]}$.

The numerical inputs

We update the LDMEs in units of GeV^3 by including the p_T shift effects in χ_{cJ} and $\psi(2S)$ production and Branch functions from higher states to J/ψ is taken from PDG 2018.

$$\begin{aligned} \mathcal{O}^{J/\psi}(^3S_1^{[1]}) &= 1.16, \quad \mathcal{O}^{J/\psi}(^3S_1^{[8]}) = 1.25 \times 10^{-3}, \quad \mathcal{O}^{J/\psi}(^1S_0^{[8]}) = 3.6 \times 10^{-2}, \\ \mathcal{O}^{J/\psi}(^3P_0^{[8]}) &= 0, \quad \mathcal{O}^{\psi'}(^3S_1^{[1]}) = 0.76, \quad \mathcal{O}^{\psi'}(^3S_1^{[8]}) = 3.41 \times 10^{-4}, \\ \mathcal{O}^{\psi'}(^1S_0^{[8]}) &= 2.19 \times 10^{-3}, \quad \mathcal{O}^{\psi'}(^3P_0^{[8]}) = 0, \quad \mathcal{O}^{\chi_{c0}}(^3P_0^{[1]})/m_c^2 = 4.77 \times 10^{-2}, \\ \mathcal{O}^{\chi_{c0}}(^3S_1^{[8]}) &= 5.29 \times 10^{-4}, \quad \text{Br}(\chi_{c1} \rightarrow J/\psi\gamma) = 34.4\%, \\ \text{Br}(\chi_{c2} \rightarrow J/\psi\gamma) &= 19.0\%, \quad \text{and} \quad \text{Br}(\psi' \rightarrow J/\psi + X) = 61.4\%. \end{aligned}$$

PDF, α_s and scale set

The unintegrated PDF is generated from MRST-2008 set of collinear PDFs using Kimber-Martin-Ryskin(KMR) scheme, and the corresponding running of α_s . The default choice of factorization and renormalization

$$\text{scale is } \mu_r = \mu_f = m_T = \sqrt{(4m_c)^2 + \bar{p}_T^2}$$

- Recall the CMS kinematic cut conditions:

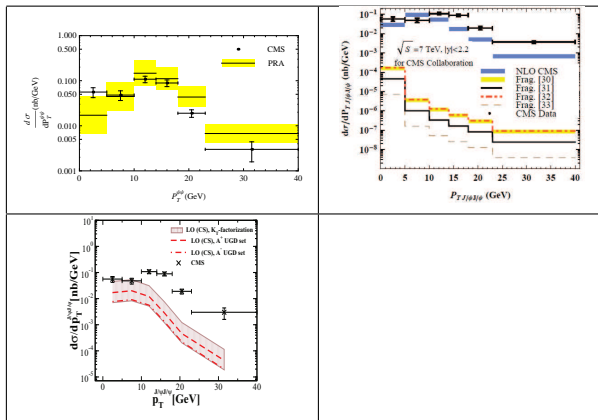
$$\begin{aligned} p_T^{J/\psi} > 4.5 \text{ GeV} & \quad \text{if } 1.43 < |y^{J/\psi}| < 2.2, \\ 4.5 \text{ GeV} < p_T^{J/\psi} < 6.5 \text{ GeV} & \quad \text{if } 1.2 < |y^{J/\psi}| < 1.43, \\ p_T^{J/\psi} > 6.5 \text{ GeV} & \quad \text{if } |y^{J/\psi}| < 1.2. \end{aligned}$$

- Total cross section:

$$\begin{aligned} \sigma^{CMS} &= (1.49 \pm 0.07 \pm 0.13) \text{ nb}, \sigma_{LO}^{PRA} = 0.84_{-0.39}^{+0.66} \text{ nb}, \\ \sigma_{LO}^{CPM} &= 0.15 \text{ nb}, \sigma_{NLO(CS^*)}^{CPM} = 0.98 \pm 0.16 \text{ nb} \end{aligned}$$

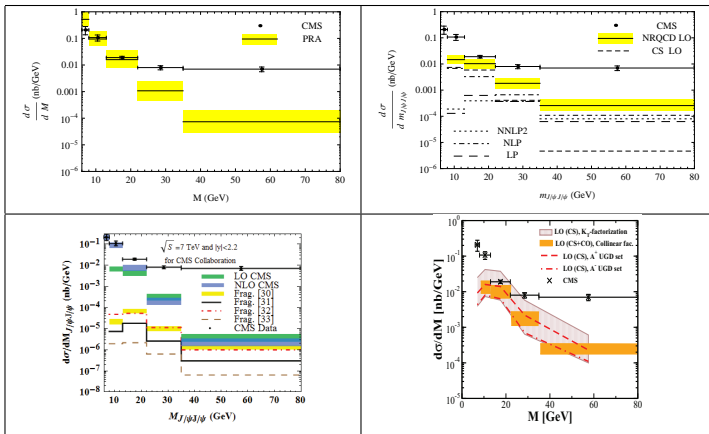
Comparison with CMS data II

- Compare PRA+NRQCD@LO (up-left), CPM+CSM@NLO (up-right), and k_t +NRQCD@LO (down-left) predictions with CMS data for the spectrum of J/ψ pair transverse momentum:



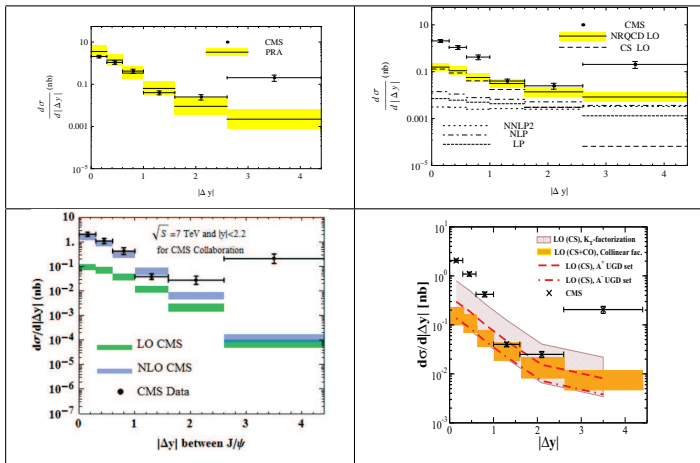
Comparison with CMS data III

- Compare PRA+NRQCD@LO (up-left), CPM+NRQCD@LO (up-right), CPM+CSM@NLO (down-left), k_t +NRQCD@LO (down-right) predictions with CMS data for the invariant mass spectrum:



Comparison with CMS data IV

- Compare PRA+NRQCD@LO (up-left), CPM+NRQCD@LO (up-right), CSM@NLO (down-left), and k_t +NRQCD@LO (down-right) predictions with CMS data for the $|\Delta y|$ distribution:



Comparison with ATLAS data I

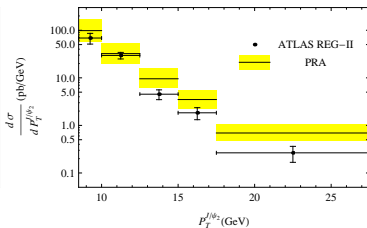
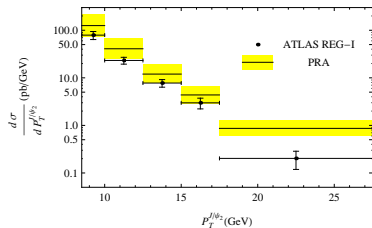
- ATLAS measured $2J/\psi$ production with cut conditions $p_T^{J/\psi} > 8.5$ GeV and $|y^{J/\psi}| < 2.1$, and they split the total cross section and differential cross section into the central rapidity region $|y(J/\psi_2)| < 1.05$ and non-central rapidity region $1.05 < |y(J/\psi_2)| < 2.1$ of the sub-leading J/ψ .
- Total cross section:

$$\sigma(pp \rightarrow J/\psi J/\psi + X) = \begin{cases} 82.2 \pm 8.3 \text{ (stat)} \pm 6.3 \text{ (syst)} \pm 0.9 \text{ (BF)} \pm 1.6 \text{ (lumi)} \text{ pb, for } |y| < 1.05, \\ 78.3 \pm 9.2 \text{ (stat)} \pm 6.6 \text{ (syst)} \pm 0.9 \text{ (BF)} \pm 1.5 \text{ (lumi)} \text{ pb, for } 1.05 \leq |y| < 2.1. \end{cases}$$

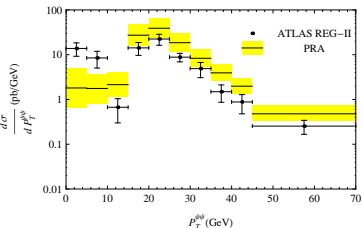
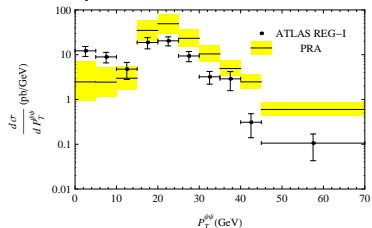
$$\sigma_{\text{ATLAS}}^{\text{PRA}} = \begin{cases} 66.8_{-26.1}^{+44.8} \text{ pb, for } |y(J/\psi_2)| < 1.05 \\ 52.6_{-20.8}^{+36.9} \text{ pb, for } 1.05 < |y(J/\psi_2)| < 2.1 \end{cases}$$

Comparison with ATLAS data II

- The $p_T(J/\psi_2)$ distribution:

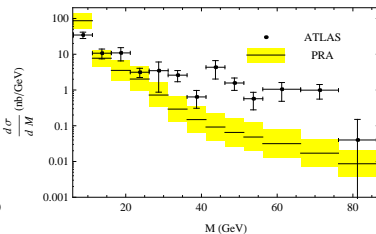
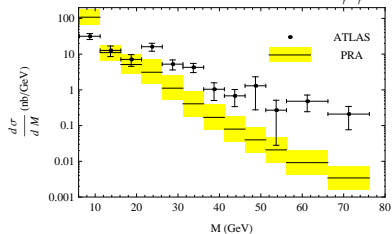


- The $p_T^{\psi\psi}$ distribution:



Comparison with ATLAS data III

- The invariant mass $M = m_{\psi\psi}$ distribution:



Further investigation between CPM, PRA and “old” k_T I

- The above results show that in low $m_{\psi\psi}$ and small $|\Delta y|$ region, PRA results are much larger than those of CPM by a factor about $5 \sim 6$, while the results of old k_T are similar to CPM.
- In large $m_{\psi\psi}$ and $|\Delta y|$ region, the predictions of CPM, PRA and old k_T are similar.

The gauge invariant amplitude is necessary in the low $m_{\psi\psi}$ and small $|\Delta y|$ region, while in large $m_{\psi\psi}$ and $|\Delta y|$ it might be irrelevant.

Note

In such regions, the LT subprocess in PRA contribute predominately, so do the same final states pairings in CPM calculation.

- We define $K_{m,n}^M = \frac{d\sigma_{m,n}^{\text{PRA}}/dm_{\psi\psi}}{d\sigma_{m,n}^{\text{CPM}}/dm_{\psi\psi}}$ and $K_{m,n}^Y = \frac{d\sigma_{m,n}^{\text{PRA}}/d|\Delta y|}{d\sigma_{m,n}^{\text{CPM}}/d|\Delta y|}$, and calculate their values for the last $m_{\psi\psi}$ and $|\Delta y|$ bins in CMS measurements.

TABLE II: The $K_{m,n}^M$ ($K_{m,n}^Y$) for the last $m_{\psi\psi}$ ($|Y|$) bins in CMS measurements.

(m, n)	${}^3S_1^{[1]}$	${}^3S_1^{[8]}$	${}^1S_0^{[8]}$	${}^3P_1^{[1]}$	${}^3P_2^{[1]}$
${}^3S_1^{[1]}$	1.12 (1.5)	1.66(3.34)	0.91(2.27)	—	—
${}^3S_1^{[8]}$	—	1.08(1.21)	0.63(0.73)	0.59(0.68)	0.91(1.11)
${}^1S_0^{[8]}$	—	—	0.54(0.6)	0.47(0.54)	0.86(1.03)
${}^3P_1^{[1]}$	—	—	—	0.43(0.49)	0.76(0.9)
${}^3P_2^{[1]}$	—	—	—	—	1.64 (2.0)

- The double prompt J/ψ hadroproduction is studied in Parton Reggeization Approach by including feed-down contribution from the higher excited states χ_{cJ} and ψ' .
- The PRA predictions of the total cross sections agree with both CMS and ATLAS measurements.
- The PRA calculation can also well explain the $p_T^{\psi\psi}$ distribution for both CMS and ATLAS sets up and $P_T(J/\psi_2)$ distribution measured by ATLAS Collaboration.
- However, there are still large discrepancies between PRA predictions and CMS and ATLAS data of the invariant mass $m_{\psi\psi}$ distribution in large $M_{\psi\psi}$ region.

History of factorization

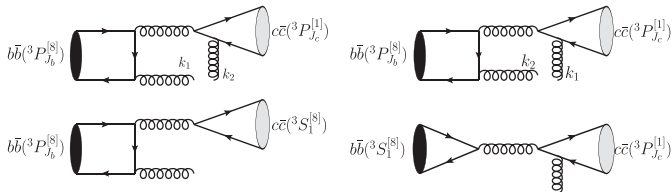
- In the CS model, originally it was found that in P -wave states decay at LO and relativistic corrections to S -wave states decay at NLO (R.Barbieri et al. 1976) there are uncancelled infrared divergence, and then extended to general cases of $L > 1$ (Belanger et al. 1981).
- This problem is solved by NRQCD factorization formalism, in which the infrared divergence is absorbed into the CO LDMEs (BBL 1995).
- Later, it is found that in the exclusive decay of $\chi_{cJ} \rightarrow l^+l^-$ (Yang et al. 2012) and production of χ_{cJ} in B-meson decay (Song et al. 2004) and double charmium production in e^+e^- annihilation (Bodwin et al. 2008) there are also uncancelled infrared divergences.
- In the exclusive processes, the infrared divergence appears in the loop integration of virtual corrections. They either disappear in the limit of $m_c/m_b(\sqrt{s}) \rightarrow 0$ or can be solved in pNRQCD (Beneke et al. 2009).

New type infrared divergence in $\Upsilon \rightarrow \text{charmonium} + X$

- The NRQCD factorization formalism for $\Upsilon \rightarrow H + X$ with $H = \eta_c, J/\psi, \chi_{cJ}, \dots$

$$\Gamma(\Upsilon \rightarrow H + X) = \sum_{m,n} \hat{\Gamma}(b\bar{b}(m) \rightarrow c\bar{c}(n) + X) \langle \Upsilon | \mathcal{O}(m) | \Upsilon \rangle \langle \mathcal{O}^H(n) \rangle.$$

- In single P -wave case, whether m or n is P -wave, the infrared divergence can be absorbed into the NRQCD LDMEs.
- But not the case when both m and n are in P -wave state. For simplicity, we show $b\bar{b}(^3P_{J_b}^{[8]}) \rightarrow c\bar{c}(^3P_{J_c}^{[1]}) + gg$.



$$b\bar{b}(^3P_J^{[8]}) \rightarrow c\bar{c}(^3P_1^{[1]}) + gg \quad |$$

- We calculate the SDC directly by implementing the covariant spin project method, and do the phase space integration for the soft region analytically.
- We divided the results into 3 parts, i.e $\Gamma^{\text{div}}(J_C) = \Gamma_1^{\text{div}} + 9\Gamma_2^{\text{div}}(J_C) + \Gamma_3^{\text{div}}(J_C)$, where

$$\hat{\Gamma}_1^{\text{div}} = \frac{-8\alpha_s}{27\pi m_c^2} \frac{1}{\epsilon_{\text{IR}}} \times \frac{5\pi^2\alpha_s^3(3r^4 + 2r^2 + 7)}{72m_b^7 r^3(1-r^2)},$$

$$\hat{\Gamma}_2^{\text{div}}(J_C) = \frac{-5\alpha_s}{9\pi m_b^2} \frac{1}{\epsilon_{\text{IR}}} \times \begin{cases} \frac{\pi^2\alpha_s^3(1-3r^2)^2}{81m_b^7 r^3(1-r^2)}, & J_C = 0, \\ \frac{2\pi^2\alpha_s^3(r^2+1)}{81m_b^7 r^3(1-r^2)}, & J_C = 1, \\ \frac{2\pi^2\alpha_s^3(6r^4+3r^2+1)}{405m_b^7 r^3(1-r^2)}, & J_C = 2, \end{cases}$$

$$b\bar{b}(^3P_J^{[8]}) \rightarrow c\bar{c}(^3P_1^{[1]}) + gg \quad ||$$

• and

$$\hat{\Gamma}_3^{\text{div}}(0) = -\frac{10\pi\alpha_s^4}{81m_b^9 r^3 (1-r^2)^4 \epsilon_{\text{IR}}} \times (3r^4 - 10r^2 + 3) (r^4 - 4r^2 \ln r - 1),$$

$$\hat{\Gamma}_3^{\text{div}}(1) = \frac{10\pi\alpha_s^4}{81m_b^9 r^3 (1-r^2)^4 \epsilon_{\text{IR}}} [-r^6 + 9r^4 - 7r^2 + 4r^2 (r^4 - 3r^2 - 2) \ln r - 1],$$

$$\hat{\Gamma}_3^{\text{div}}(2) = \frac{2\pi\alpha_s^4}{81m_b^9 r^3 (1-r^2)^4 \epsilon_{\text{IR}}} [6r^8 + 23r^6 - 27r^4 + r^2 - 4r^4 (9r^2 + 11) \ln r - 3],$$

with $r = m_c/m_b$.

$$b\bar{b}(^3P_J^{[8]}) \rightarrow c\bar{c}(^3P_1^{[1]}) + gg \quad \text{III}$$

- The origin of Γ_1^{div} is from soft gluon only emitted and absorbed by charm (anti-)quark so it can be absorbed by the NLO QCD corrections to the LDME $\langle \mathcal{O}^{\chi_{cJ}}(^3S_1^{[8]}) \rangle$ in $b\bar{b}(^3P_{J_b}^{[8]}) \rightarrow c\bar{c}(^3S_1^{[8]}) + g$.
- The origin of $\Gamma_2^{\text{div}}(J_c)$ is from soft gluon only emitted and absorbed by bottom (anti-)quark so can be absorbed by the NLO QCD corrections to the LDME $\langle \Upsilon | \mathcal{O}(^3S_1^{[8]}) | \Upsilon \rangle$ in $b\bar{b}(^3S_1^{[8]}) \rightarrow c\bar{c}(^3P_{J_c}^{[1]}) + g$.
- However the origin of $\Gamma_3^{\text{div}}(J_c)$ is from soft gluon emitted and absorbed by different heavy quarks. There is no LDMEs to describe such effect yet!

Unlike in the exclusive P-wave production case, $\Gamma^3(J_c)$ do not vanish in the limit $r \rightarrow 0$!

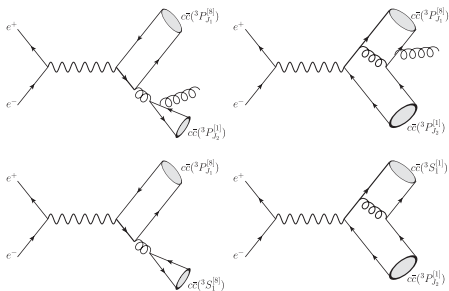
More general case

- Since $\Gamma_3^{\text{div}}(J_c)$ is due to the interference of diagrams with soft gluon emission by P-wave $b\bar{b}$ and $c\bar{c}$ Fock states, which can appear in NRQCD treatment of inclusive decay process of bottomonium into charmonium. We conclude generally NRQCD factorization will breakdown for any such process at some order of v_c^2 and v_b^2 .
- In particular, for χ_{cJ} production in χ_{bJ} decay, it happens at LO of v_b^2 and v_c^2 .

What will happen for the case of 2 charmonia production especially at hadron collider?

$$e^+e^- \rightarrow c\bar{c}(^3P_J^{[8]}) + c\bar{c}(^3P_J^{[1]}) + g$$

- For prompt double J/ψ hadroproduction, the soft gluon emission starts at QCD NLO in α_s , e.g., $gg \rightarrow c\bar{c}(^3P_{J_1}^{[8]}) + c\bar{c}(^3P_{J_2}^{[8]}) + g$.
- There will be additional infrared divergence to be cancelled by virtual corrections, which make it very much difficult to calculate.
- Alternatively, we choose the $J/\psi + \chi_{cJ}$ production in e^+e^- annihilation through $e^+e^- \rightarrow c\bar{c}(^3P_J^{[8]} + c\bar{c}(^3S_1^{[8]})) + g$ as illustration, the representative feynman diagrams for which is:



$$e^+e^- \rightarrow c\bar{c}({}^3P_J^{[8]}) + c\bar{c}({}^3P_J^{[1]}) + g \parallel$$

- Again, we found there are also 3 sources of the infrared divergence:
 - The squared amplitude in which gluon attached to $c\bar{c}({}^3P_J^{[8]})$: σ_1^{div}
 - The squared amplitude in which gluon attached to $c\bar{c}({}^3P_1^{[1]})$: $\sigma_2^{\text{div}}(J_2)$
 - The interference term between the above 2 parts amplitude: $\sigma_3^{\text{div}}(J_2)$
- The total result is:

$$\sigma^{\text{div}} = \sigma_1^{\text{div}} + 9\sigma_2^{\text{div}}(J_2) + \sigma_3^{\text{div}}(J_2)$$

where

$$\hat{\sigma}_1^{\text{div}} = -\frac{8\alpha_s}{27\pi m_c^2} \frac{1}{\epsilon_{\text{IR}}} \frac{2^{10}\pi^3\alpha^2\alpha_s^2\mathcal{S}}{729s^5r^6} \times (864r^{10} - 144r^8 - 1568r^6 + 1224r^4 - 130r^2 + 27),$$

$$e^+ e^- \rightarrow c\bar{c}({}^3P_J^{[8]}) + c\bar{c}({}^3P_J^{[1]}) + g \text{ III}$$

$$\hat{\sigma}_2^{\text{div}}(J_2) = -\frac{4\alpha_s}{3\pi m_c^2 \epsilon_{\text{IR}}} \times \frac{2^{18} \pi^3 \alpha^2 \alpha_s^2 S}{19683 s^5 r^4}$$

$$\begin{cases} (144r^8 + 152r^6 - 428r^4 + 182r^2 + 1), & J_2 = 0, \\ 8(18r^6 + 13r^4 - 12r^2 + 2), & J_2 = 1, \\ \frac{2}{5}(360r^8 + 308r^6 - 188r^4 + 20r^2 + 1), & J_2 = 2, \end{cases}$$

$$\hat{\sigma}_3^{\text{div}}(0) = \frac{2^{19} \pi^2 \alpha^2 \alpha_s^3}{3^8 s^6 r^4 \epsilon_{\text{IR}}} \times [(144r^8 + 184r^6 - 504r^4 + 170r^2 + 33) S$$

$$+ 8(72r^{10} + 56r^8 - 284r^6 + 149r^4 + r^2) T],$$

$$e^+ e^- \rightarrow c\bar{c}(^3P_J^{[8]}) + c\bar{c}(^3P_J^{[1]}) + g \text{ IV}$$

$$\hat{\sigma}_3^{\text{div}}(1) = \frac{2^{19}\pi^2\alpha^2\alpha_s^3}{3^8 s^6 r^2 \epsilon_{\text{IR}}} \times [(144r^6 + 28r^4 - 176r^2 + 43) S \\ + (576r^{10} - 176r^8 - 792r^6 + 424r^4 - 48r^2) T],$$

$$\hat{\sigma}_3^{\text{div}}(2) = \frac{2^{19}\pi^2\alpha^2\alpha_s^3}{5 \cdot 3^8 s^6 r^4 \epsilon_{\text{IR}}} [(720r^8 + 452r^6 - 696r^4 + 7r^2 - 15) S \\ + (2880r^{10} + 368r^8 - 3560r^6 + 1856r^4 - 56r^2) T],$$

where $r = 2m_c/\sqrt{s}$, $S = \sqrt{1 - 4r^2}$, and $T = \tanh^{-1} S$.

$$e^+e^- \rightarrow c\bar{c}(^3P_J^{[8]}) + c\bar{c}(^3P_J^{[1]}) + g V$$

- σ_1^{div} is cancelled after including NLO QCD corrections to LDME $\langle \mathcal{O}^{\chi_{cJ}}(^3S_1^{[8]}) \rangle$ of $e^+e^- \rightarrow c\bar{c}(^3P_J^{[8]}) + c\bar{c}(^3S_1^{[8]})$.
- $\sigma_2^{\text{div}}(J_2)$ is cancelled after including NLO QCD corrections to LDME $\langle \mathcal{O}^{J/\psi}(^3S_1^{[1]}) \rangle$ of $e^+e^- \rightarrow c\bar{c}(^3S_1^{[1]}) + c\bar{c}(^3P_J^{[1]})$.
- $\hat{\sigma}_3^{\text{div}}(J_2)$ is left!
- The behaviors of σ_i^{div} as r goes to 0 are: $\sigma_1^{\text{div}} \propto \frac{1}{r^7}$,
 $\sigma_2^{\text{div}} \propto \frac{1}{r^5}, \sigma_3^{\text{div}} \propto \frac{1}{r^4}$.
- Although the new type of singularities will not disappear, in the limit of $r \rightarrow 0$, they are less singular.

- The new type divergence originates from the interference of Feynman diagrams where soft gluon attached to different $Q\bar{Q}$ states independent on the initial states and not requiring the 2 quark pairs be the same flavor.
- We predict that this new type divergence will also appears in the calculation of NLO QCD corrections for double J/ψ and $J/\psi + \Upsilon$ hadroproduction.
- However, the structure of the new type divergence can be more complicated, because more channels are involved.
- For $gg \rightarrow c\bar{c}(^3P_{J_c}^{[8]}) + b\bar{b}(^3P_{J_b}^{[8]}) + g$, there will be 4 pairing $c\bar{c}(^3S_1^{[8]}) + b\bar{b}(^3P_{J_b}^{[8]})$, $c\bar{c}(^3S_1^{[1]}) + b\bar{b}(^3P_{J_b}^{[8]})$, $c\bar{c}(^3P_{J_c}^{[8]}) + b\bar{b}(^3S_1^{[1]})$, and $c\bar{c}(^3P_{J_c}^{[8]}) + b\bar{b}(^3S_1^{[8]})$, which lead to more interference terms.

Basic idea to solve the problem I

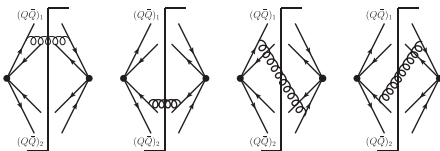
- Recall that factorization implies a complete separation of perturbative and non-perturbative effects.
- Our prime goal is to first find a way to separate the IR singular terms like $\Gamma_3^{\text{div}}(J_C)$ and $\sigma_3^{\text{div}}(J_2)$ into contributions pertaining to the hard- and soft-scale regimes.
- Since now the 2 pairs can not be at rest simultaneously, we need the covariant form of NRQCD Lagrangian:

$$\begin{aligned}\mathcal{L}_{\text{NRQCD}}^{\text{LO}} &= \bar{\psi}_v \left[iv \cdot D + \frac{(iD_{\top}^{\mu})(iD_{\top\mu})}{2m} \right] \psi_v \\ &+ \bar{\chi}_v \left[-iv \cdot D + \frac{(iD_{\top}^{\mu})(iD_{\top\mu})}{2m} \right] \chi_v,\end{aligned}$$

where m is heavy quark mass $v^{\mu} = p^{\mu}/m$ with p^{μ} the momentum of $Q\bar{Q}$ pair.

Basic idea to solve the problem II

- ψ_v and χ_v are the nonrelativistic heavy-quark and -antiquark in four component form satisfying $\not{v}\psi_v = \psi_v$ and $\not{v}\chi_v = -\chi_v$.
- The \perp component of a vector a^μ is defined as: $a_\perp^\mu = a^\mu - v^\mu v \cdot a$.
- The creation and annihilation of heavy quark pair surely take place in short-distance. We then can depict the diagrams for the one loop corrections as:



- The interference effect is described by the last 2 panels.

Basic idea to solve the problem III

- To describe the vertex we introduce the new operators:

$$\psi_{b,v_1} \mathcal{K}^{\mu_1\nu_1} T^{a_1} \bar{\chi}_{b,v_1} \bar{\psi}_{c,v_2} \gamma_T^{\nu_2} T^{a_2} \chi_{c,v_2}, \quad \psi_{b,v_1} \gamma_T^{\nu_1} T^a \bar{\chi}_{b,v_1} \bar{\psi}_{c,v_2} \mathcal{K}_J^{\mu_2\nu_2} \chi_{c,v_2}$$

and their charge conjugates for $b\bar{b}({}^3P_{J_b}^{[8]}) \rightarrow c\bar{c}({}^3P_J^{[1]}) + gg$ and

$$\bar{\psi}_{c,v_1} \mathcal{K}^{\mu_1\nu_1} T^{a_1} \chi_{c,v_1} \bar{\psi}_{c,v_2} \gamma_T^{\nu_2} T^{a_2} \chi_{c,v_2}, \quad \bar{\psi}_{c,v_1} \gamma_T^{\nu_1} \chi_{c,v_1} \bar{\psi}_{c,v_2} \mathcal{K}_J^{\mu_2\nu_2} \chi_{c,v_2}$$

and their charge conjugates for $e^+e^- \rightarrow c\bar{c}({}^3P_{J_1}^{[8]}) + c\bar{c}({}^3P_{J_2}^{[1]}) + g$.

- The definition of \mathcal{K} s are: $\mathcal{K}_0^{\mu\nu} = \frac{g^{\mu\nu} - v^\mu v^\nu}{\sqrt{3}} (-\frac{i}{2} \overleftrightarrow{\mathcal{D}}_T)$,

$$\mathcal{K}_1^{\mu\nu} = \frac{-i}{2} (\overleftrightarrow{\mathcal{D}}_T^{[\mu} \gamma_T^{\nu]}), \quad \mathcal{K}_2^{\mu\nu} = \frac{-i}{2} (\overleftrightarrow{\mathcal{D}}_T^{(\mu} \gamma_T^{\nu)}), \quad \text{and } \mathcal{K}^{\mu\nu} = \frac{-i}{2} (\overleftrightarrow{\mathcal{D}}_T^{\mu} \gamma_T^{\nu})$$

with $a^{[\mu} b^{\nu]} = \frac{1}{2}(a^\mu b^\nu - a^\nu b^\mu)$ and

$$a^{(\mu} b^{\nu)} = \frac{1}{2}(a^\mu b^\nu + a^\nu b^\mu) - \frac{g^{\mu\nu} - v^\mu v^\nu}{3} a \cdot b.$$

One loop corrections of soft gluon

- Derive the feynman rule from the Lagrangian, we then can calculate the loop integrals. For example, for the third pannel:

$$I = -ig_s^2 \mu^{4-D} \int \frac{d^D l}{(2\pi)^D} \times \frac{\left[v_1 + \frac{(2q_1+l)_T}{2m_1} \right] \cdot \left[v_2 + \frac{(2q_2+l)_T}{2m_2} \right]}{l^2 \left[l \cdot v_1 + \frac{(l+q_1)_T^2}{2m_1} \right] \left[l \cdot v_2 + \frac{(l+q_2)_T^2}{2m_2} \right]}.$$

- Although numerically m_b is 3 times larger than m_c , we assume that $m_c \gg m_b v_b$ to ensure the nonrelativistic approximation for m_c still applies.
- Expand the integrand in series of $1/m_i$ and dropping terms of $1/m_i^2$ and higher orders.

One loop corrections of soft gluon

- We get

$$I = I_0 + \frac{\alpha_s \mu^{4-D}}{\pi m_1 m_2} \left(\frac{1}{\epsilon_{UV}} - \frac{1}{\epsilon_{IR}} \right) \times \left[\frac{\ln(\omega + \sqrt{\omega^2 - 1}) - \omega \sqrt{\omega^2 - 1}}{2(\omega^2 - 1)^{3/2}} \times q_1 \cdot q_2 + \frac{(\omega^2 + 2)\sqrt{\omega^2 - 1} - 3\omega \ln(\sqrt{\omega^2 - 1} + \omega)}{2(\omega^2 - 1)^{5/2}} \times (v_1 \cdot q_2)(v_2 \cdot q_1) \right],$$

where $\omega = v_1 \cdot v_2$

- After we sum over contribution of all the diagrams I_0 , which is irrelevant, will disappear.

One loop corrections of soft gluon

- The loop integrals are process independent although the results depends on ω .
- The ultraviolet divergence can be removed through operator renormalization.
- Multiplying the corresponding SCDs, and decomposing the tensor and color structures into basis of total-angular momentum and color states.
- The IR-singular parts exactly matches those in $\Gamma_3^{\text{div}}(J_c)$ and $\sigma_3^{\text{div}}(J_2)$, respectively!
- This implies it is possible to construct a general factorization formalism within NRQCD to describe processes involving 2 or more heavy quarkonia.

- We illustrated via 2 examples $\Upsilon \rightarrow \chi_{cJ} + X$ and $e^+e^- \rightarrow J/\psi + \chi_{cJ} + X$ that there are uncancelled infrared divergences in standard NRQCD factorization calculation.
- We extended the conclusion to any subprocess involving 2 P -wave Fock states.
- We introduced new type of operators and shown that their NLO QCD corrections can precisely reproduce the uncancelled infrared divergence.
- Much more further works are needed to construct a generalized NRQCD factorization formalism and to investigate its phenomenology influence, especially for double quarkonia hadroproduction.

Thank you !